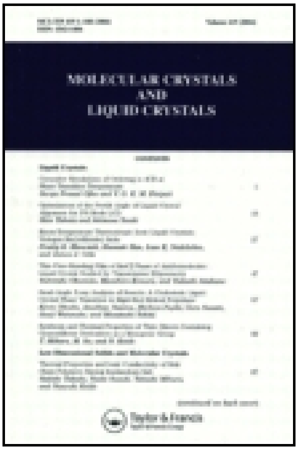

Molecular Crystals and Liquid Crystals

Publication details, including instructions for authors and subscription information:
http://www.tandfonline.com/loi/gmcl20

Dynamics of Cyanophenyl Alkylbenzoate Molecules in a Surface Layer Adsorbed onto Aerosil. I. Cyanophenyl Hexylbenzoate

Stefan Frunza [a] , Andreas Schönhals [b] , Harald Goering [b] , Doina Manaila-Maximean [c] , Traian Beica [a] , Ligia Frunza [a] & Rodica Moldovan [d]

[a] National Institute of Materials Physics, Magurele, Romania

[b] Federal Institute of Materials Research and Testing, Berlin, Germany

[c] University "Politehnica Bucuresti", Bucharest, Romania

[d] Romanian Academy Center of Advanced Studies in Physics, Bucharest, Romania

To cite this article: Stefan Frunza, Andreas Schönhals, Harald Goering, Doina Manaila-Maximean, Traian Beica, Ligia Frunza & Rodica Moldovan (2008): Dynamics of Cyanophenyl Alkylbenzoate Molecules in a Surface Layer Adsorbed onto Aerosil. I. Cyanophenyl Hexylbenzoate, Molecular Crystals and Liquid Crystals, 495:1, 60/[412]-79/[431]

To link to this article: http://dx.doi.org/10.1080/15421400802430448

Mol. Cryst. Liq. Cryst., Vol. 495, pp. 60/[412]–79/[431], 2008
Copyright © Taylor & Francis Group, LLC
ISSN: 1542-1406 print/1563-5287 online
DOI: 10.1080/15421400802430448

Dynamics of Cyanophenyl Alkylbenzoate Molecules in a Surface Layer Adsorbed onto Aerosil. I. Cyanophenyl Hexylbenzoate

Stefan Frunza[1], Andreas Schönhals[2], Harald Goering[2], Doina Manaila-Maximean[3], Traian Beica[1], Ligia Frunza[1], and Rodica Moldovan[4]
[1]National Institute of Materials Physics, Magurele, Romania
[2]Federal Institute of Materials Research and Testing, Berlin, Germany
[3]University "Politehnica Bucuresti", Bucharest, Romania
[4]Romanian Academy Center of Advanced Studies in Physics, Bucharest, Romania

A composite prepared from aerosil A380 and the liquid crystal (LC) 4-hexyl-4′-cyanophenyl benzoate (CP6B) was investigated by broadband dielectric spectroscopy in a large temperature range. The selected high silica density (ca. 7g aerosil/1 g of CP6B) allows the observation of a thin layer (two-monolayer structure) adsorbed on the surface of the silica particles. For the composite one relaxation process is observed at frequencies much lower than that of the processes found for bulk CP6B. It is assigned to the dynamics of the molecules in the surface layer. The temperature dependence of its relaxation rates obeys the Vogel–Fulcher–Tammann law, which is characteristic for glass-forming liquids. The quasi 2D character of the observed glassy dynamics in the surface layer is discussed. The temperature dependence of the CP6B relaxation in the composite is compared with that of related hexylcyanobiphenyl molecules in the surface layer of aerosil composite with a similar concentration.

Keywords: aerosil composites; cyanophenyl-alkylbenzoates; dielectric spectroscopy; infrared spectroscopy; liquid crystals; thermal analysis

SF, LF, TB, RM and DMM gratefully acknowledge the financial support from Romanian Ministry of Education and Research (Project CEEX 76/C1). LF and SF are also grateful for their fellowships from Federal Institute of Materials Research and Testing (BAM). The authors thank Degussa-Hüls for the aerosil samples.

Address correspondence to Stefan Frunza, National Institute of Materials Physics, Magurele R-077125, Romania. E-mail: frunza@infim.ro

INTRODUCTION

Cyanobiphenyl (CB) – aerosil composites were recently used as model systems to study the molecular motions of a surface layer of cyanobiphenyl molecules by broadband dielectric spectroscopy. The investigations were performed for high silica densities [1] in order to study only the behavior of the molecules, which are adsorbed onto the surface of the silica particles. A bulk-like relaxation of the bulk CB molecules was observed especially for samples with low silica densities ([1] and references herein). But for composites with high silica densities only a slow relaxation process was detected which shows no discontinuities at the phase transitions of the bulk liquid crystal (LC). This relaxation process was observed even at temperatures for which bulk CB is in the crystalline state. It was assigned to the surface layer of CB molecules.

Liquid crystals from the 4-*n*-alkyl-4′-cyanophenyl benzoate homologous series and their composites are much less studied than those from the CB series despite the fact that their interactions with a surface can be richer than that in the CB case. This contribution presents first results for composites containing aerosil and 4-*n*-hexyl-4′-cyanophenyl benzoate (CP6B, 6 carbon atoms in the alkyl chain) as obtained by broadband dielectric spectroscopy. Comparison is made with the behavior obtained for the corresponding bulk CP6B in the liquid crystalline and isotropic state and for composites containing 6CB (4-*n*-hexyl-4′-cyanobiphenyl) with a similar composition. The dielectric investigations were supported by IR spectroscopy and thermal analysis.

EXPERIMENTAL

The structure of 4-*n*-hexyl-4′-cyanophenyl benzoate is given below:

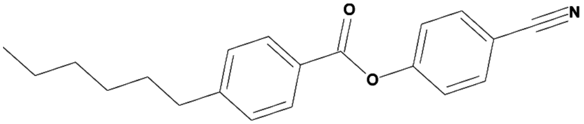

it was purchased from Roche (Basel, Switzerland) and used without further purification. The temperature of the phase transitions during the heating are given in the literature as follows [2–6]

$$\mathrm{Cr}\ 317.5\,\mathrm{K} - \mathrm{N}\ 321.7\,\mathrm{K} - \mathrm{I}$$

where Cr symbolizes the crystalline, N the nematic and I the isotropic state.

The hydrophilic aerosil (type A380, Degussa-Hüls) was used after drying under vacuum at ~500 K for at least 12 h. This aerosil with a specific surface BET area of 380 m^2/g consists of silica spheres of 7 nm diameters, covered by hydroxyl groups.

Since CP6B is a solid (crystalline) at room temperature, the composites were prepared via a solution route as previously described [1,7]. In short, aerosil was firstly dried under vacuum at 500 K for at least 12 h. Then, the silica particles were mixed with a solution of CP6B dissolved in carbon tetrachloride. The solvent was carefully removed by evaporation at 348 K for 20 hours; its total removing was checked by blank experiments. High silica densities ensured to approach the case where the cyanophenyl benzoate molecules located only as a monolayer anchored on the silica particles in the composite. The ratio aerosil/CP6B of 10 has been therefore chosen. However, a partial LC evaporation/removing together with the solvent was expected and thus, the final silica density was estimated by thermogravimetry.

Dielectric spectroscopy was employed in a broad frequency (10^{-2}–10^{9} Hz) and temperature range covering the phase transitions characteristic for bulk CP6B. The equipment to measure the complex dielectric function

$$\varepsilon^*(f) = \varepsilon'(f) - i\,\varepsilon''(f) \tag{1}$$

(f-frequency, ε'-real part, ε''-loss part) was described elsewhere [8,9a]. It consists of a Novocontrol high-resolution Alpha analyzer [8] for the frequency range from 10^{-3} to 10^{7} Hz and of a coaxial reflectometer based on an impedance analyzer HP 4191A for the high frequency range (10^{6}–10^{9} Hz) [9a]. The dielectric measurements were carried out under isothermal conditions were the temperature was controlled with stability better than 0.1 K by a Novocontrol Quatro Cryosystem in the low frequency domain and by a custom made nitrogen gas jet cryostat for the high frequency regime. The temperature was increased stepwise from 200 K (much lower than the Cr/N(I) bulk phase transition) to 373 K (higher than the N/I bulk phase transition) with steps of 3 or 5 K. For bulk CB6B the measurements are carried out for a non-aligned sample were fused silica fibbers with a diameter of 50 μm were used as spacers.

The method to analyze and to separate relaxation processes is based on the Havriliak-Negami (HN) function [9b]. The HN-function reads:

$$\varepsilon^*(f) - \varepsilon_\infty = \frac{\Delta\varepsilon}{(1 + (if/f_0)^{\beta})^{\gamma}} \tag{2}$$

where f_0 is a characteristic frequency related to the frequency of maximal loss f_p (relaxation rate) of the relaxation process under consideration, ε_∞ describes the value of the real part ε' for $f \gg f_0$. β and γ are fractional form parameters ($0 < \beta \leq 1$ and $0 < \beta\gamma \leq 1$) describing the shape of the relaxation time spectra. $\Delta\varepsilon$ denotes the dielectric strength, which is proportional to the mean squared effective dipole moment and to the number of the fluctuating dipoles per unit volume. Conduction effects were treated by adding a contribution $\sigma_0/\varepsilon_0(2\pi f)^x$ to the dielectric loss. σ_0 is related to the dc conductivity of the sample and ε_0 is the dielectric permittivity of vacuum. The parameter x ($0 < x \leq 1$) describes for $x < 1$ non-Ohmic effects in the conductivity. For details see Ref. [9b].

As the real and the imaginary part of the dielectric function are related to each other by the Kramers-Kronig relationships, meaning that both quantities carry the same information, only the dielectric loss is further considered. The results are discussed by the temperature dependence of the relaxation rate f_p and that of the dielectric strength $\Delta\varepsilon$.

The large surface-to-volume ratio of the composite samples should lead to a considerable contribution of the molecules in the surface layer to the dielectric spectra. Therefore, it was possible to get information on the dynamics and the structure of this layer.

Additional information were obtained by TG/DTA/DSC measurements and also by FTIR spectroscopy as previously described for related systems [7,10,11]. In short, the CP6B content of the composites was determined by thermogravimetric (TG) measurements, since the aerosil is (approximately) chemically stable till 1100 K, whereas the CP6B is completely oxidized and removed from the system. TG measurements were carried out simultaneously with differential thermal analysis (DTA) using a Setaram TG-DTA 92 or a Perkin Elmer Diamond apparatus under dry air, with a heating rate of 10 K/min. In addition, these measurements allow to estimate the host-guest interactions between the molecules and the surface of the matrix [10 and references herein, 12]. The thermal behavior of bulk CP6B and of the composites was studied by a differential scanning calorimeter (DSC) from Netzsch (DSC 204 F1), using scanning rates of 2, 5 or 10 K/min. Two to four heating-cooling cycles were applied for each sample.

Vibrational spectra were recorded with a Nicolet Magna 550 FTIR spectrometer on thin self-supported pellets. The spectra were analyzed by fitting Gaussians to the data as previously described [11].

RESULTS AND DISCUSSION

This paragraph is organized as follows. Firstly the properties of bulk CP6B, especially the dielectric relaxation behavior as well as those of the unloaded aerosil material are shortly described. These data are needed as reference to interpret the measurements for the CP6B-aerosil composites. After this the behavior of the CP6B molecules in the composite are discussed in detail together with that found by supplementary measurements. A detailed comparison is made with the results found for composites of similar concentration of aerosil and a cyanobiphenyl with the same length of the alkyl chain (6CB).

1. Bulk Cyanophenyl Hexylbenzoate

Thermal Analysis

CP6B forms an enantiotropic LC with a nematic mesophase. However, since the temperature range of the nematic phase is rather narrow, careful investigations are necessary to determinate it especially during heating. In cooling, the transition from the isotropic to nematic phase is well separated due to a larger hysteresis for crystallization in comparison to the mesophase transition (Fig. 1).

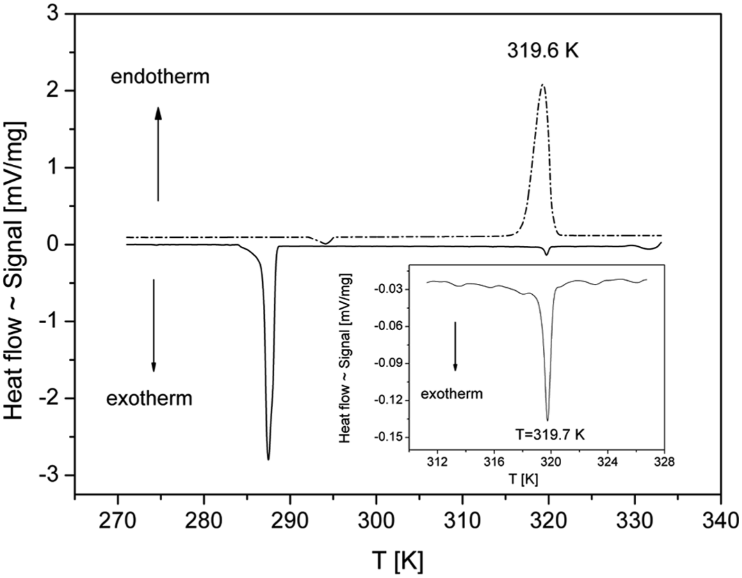

FIGURE 1 DSC curves of CP6B obtained for the first heating (dashed-dotted line) and the subsequent second cooling run (solid line) at a rate of 2 K/min. The inset enlarges the temperature range for the phase transition from the isotropic to the nematic phase during cooling.

Thermogravimetric measurements show that most of the LC amount disappears from an open pan by slowly heating it above 423 K.

FTIR Spectra

The infrared spectrum of CP6B (Fig. 2) shows strong and mostly non-overlapping bands, which can be assigned to both the rigid core and the flexible part of the molecule. Thus, at frequencies 3026–3073 cm^{-1} appear the peaks due to the $C_{arom}H$ stretch; between 2956 and 2857 cm^{-1} those due to the CH_3 and CH_2 asymmetrical and symmetrical stretch; at ~2233 cm^{-1} – CN stretch; at 1612 and 1509 cm^{-1}, – CC_{arom} stretch; at 1460, 1397 and 1378 cm^{-1} – alkyl deformation; around 1740 cm^{-1} – stretch of the carbonyl (CO) in the carboxylate group [13–19].

None of these vibrations, except probably the CN and may be the CO stretching vibration can be really described as a vibration of a localized group, since all the modes are combined modes of vibration. Therefore these stretching vibrations of the carbonyl in the ester (carboxylate) group and the cyano-groups in the rigid core of the CP6B molecule are the most appropriate to characterize the interaction of these molecules with the aerosil surface (see below).

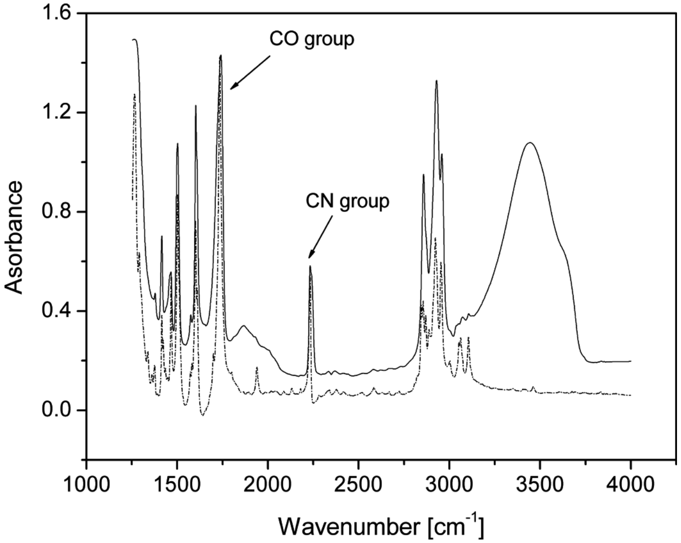

FIGURE 2 FTIR spectra for bulk CP6B (doted-dashed line) and for the composite (solid line).

Dielectric Spectroscopy

Two relaxation processes indicated by peaks were observed in the temperature range of the nematic phase and at least one broadened process in the isotropic region (Figs. 3 and 4).

The interpretation of the dielectric spectra in the nematic phase is given by the theory worked out for low molecular weight liquid crystals. LCs are anisotropic materials and therefore their dielectric properties have to be described by a tensor. For the simplest case of an uniaxial nematic phase the complex dielectric function is due to two main components of this tensor parallel $\varepsilon_{\|}^{*}(f)$ and perpendicular $\varepsilon_{\perp}^{*}(f)$ to the nematic director [9c]. Both contributions are related to different weighted sums of four underlying relaxation modes depending on the macroscopic orientation of the sample. The relaxation mode at the lowest frequencies is due to rotational fluctuations of the molecule around its short axis and determines mainly $\varepsilon_{\|}^{*}(f)$ (δ-relaxation). The other three relaxation modes (different tumbling modes of the molecules around their long axis) mainly related to $\varepsilon_{\perp}^{*}(f)$ have nearly the same relaxation rate and form a broad relaxation process observed at higher frequencies than the δ-relaxation. Extended theories predict a further relaxation process related to fluctuations of the molecules on a cone around the director [20]. Figure 4 shows one example for

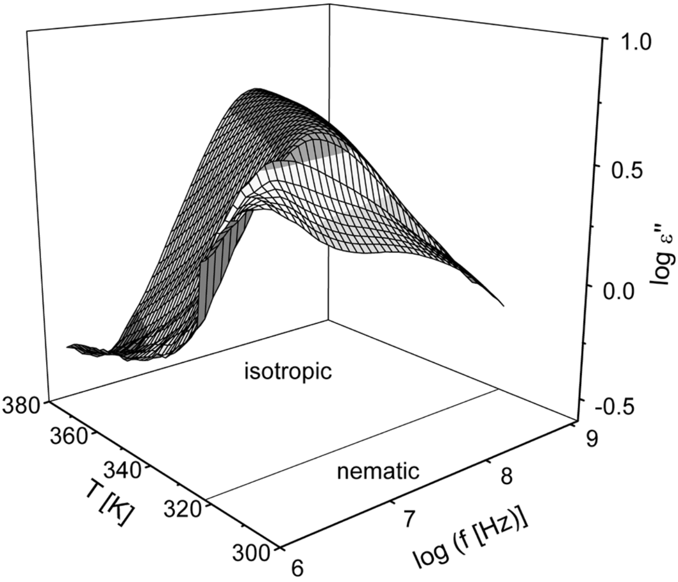

FIGURE 3 Dielectric loss vs. frequency and temperature in a 3D representation for CP6B.

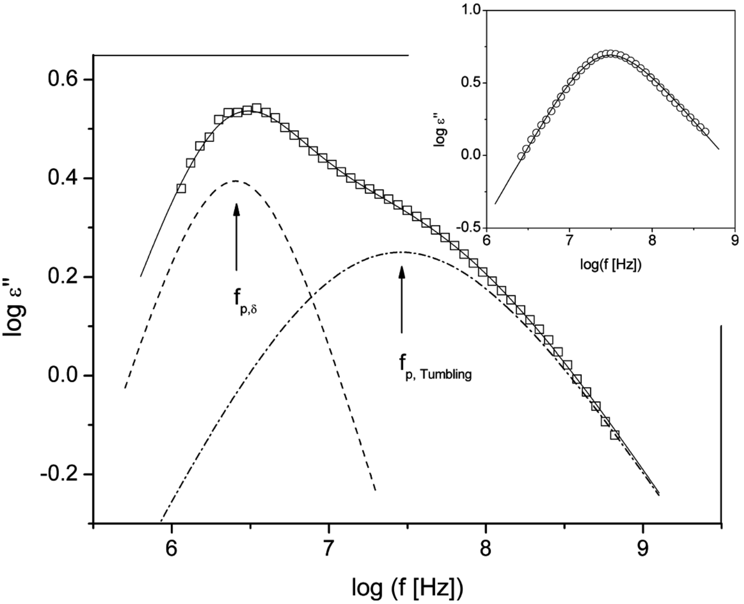

FIGURE 4 Dielectric loss vs. frequency for bulk CP6B at $T = 315.6\,K$ (nematic phase). The solid line is a fit of two HN-functions to the data. The dashed and the dashed-dotted lines are the contributions of the δ-relaxation and the tumbling mode respectively. The inset gives the dielectric loss vs. frequency in the isotropic phase at $T = 341.9\,K$. The line is a fit of the HN-function to the data.

the separation of the δ-relaxation and the tumbling mode using a fit of two HN-functions to the data. The corresponding inset gives a fit to the data in the isotropic range.

The temperature dependence of the relaxation rates for the process in the isotropic phase and for the δ-relaxation and tumbling mode in the nematic state is shown in Figure 5.

According to the theoretical approach outlined above the temperature dependence of the relaxation rates for the δ-relaxation and the tumbling modes should obey the Arrhenius law

$$f_p = f_\infty \exp[-E_A/(k_B T)] \tag{3}$$

(E_A-activation energy, f_∞-pre-exponential factor, k_B-Boltzman's constant, T-temperature).

In a limited temperature regime a dependence according to Eq. (3) is found. However, careful measurements performed over larger temperature intervals especially in the isotropic state and a more

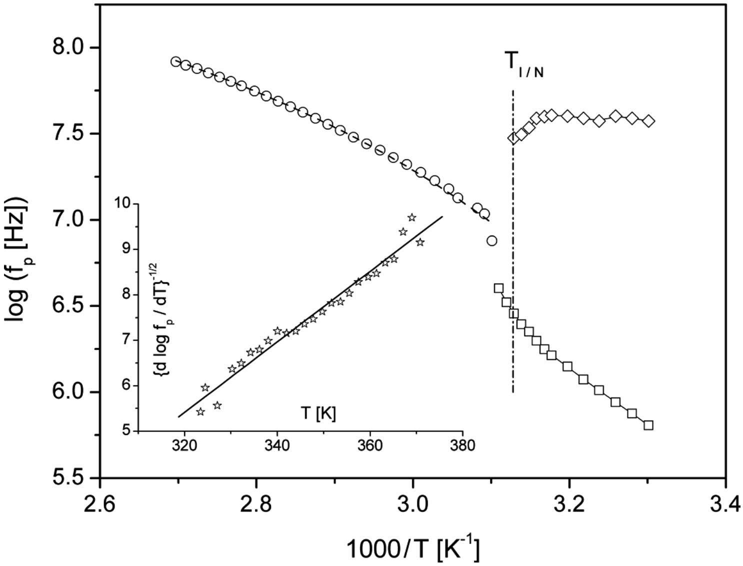

FIGURE 5 Relaxation rate f_p vs. inverse temperature for bulk CP6B measured during cooling: ○-isotropic state; □-δ-relaxation, ◇-tumbling mode. The dashed line is a fit of the VFT equation to the data taking T_0 from the derivative technique. The solid lines are guides to the eyes. The doted-dashed line indicates the phase transition temperature taken from DSC measurements during cooling. The inset shows $(d\log f_p/dT)^{-1/2}$ vs. temperature for the data in the isotropic range. The line is a linear regression to the data.

detailed analysis have shown that the temperature dependence of the relaxation rates follows the Vogel-Fulcher-Tammann (VFT) law

$$\log f_p = \log f_\infty - \frac{A}{T - T_0} \tag{4}$$

($\log f_\infty$, A-constants, T_0-so-called Vogel temperature) [9d,21]. In fact, deviations from the Arrhenius-like dependence in the temperature range of the mesophases as well as in the isotropic state were already reported [22] for CBs and other nematics. This can be proven by a more detailed analysis of the temperature dependence of the relaxation rates when a derivative method is used [9e]. This method is sensitive to the functional form of $f_p(T)$ irrespective of the prefactor. For a dependency according to the VFT-equation one gets

$$\left[\frac{d\log f_p}{dT}\right]^{-1/2} = A^{-1/2}(T - T_0). \tag{5}$$

In a plot $[d\log f_p/dT]^{-1/2}$ versus T a VFT-behavior shows up as a straight line. This method is applied to the relaxation rates of CP6B measured in the isotropic state (see inset Fig. 5). The data follow a straight line, which indicates that indeed the temperature dependence of the relaxation rates of in the isotropic state follows a VFT-dependence. The temperature dependence of the relaxation rates in the nematic state is more complex and needs extended discussions [23].

2. Aerosil

It is well known that aerosil particles are covered by surface hydroxyl groups and consequently, they can hydrogen bond to each other in a suitable medium forming a gel [24]. Since in the investigated composites the silica density is higher than a given threshold, the gel is 'rigid' and similar to an aerogel. Aerosil-based systems have a hierarchical structure consisting of different length scales. It was suggested that the individual 7 nm aerosil particles fused together during the manufacturing process to larger primary particles of ca. 20 nm [24]. These primary particles accumulate to 440 nm aggregates and even further, these aggregates forming macroscopic agglomerates. Therefore, it is expected that composite samples with high silica densities consist of aggregates and agglomerates formed by primary silica particles. This was also indicated by AFM images obtained for CB-aerosil composites [1] in agreement with the literature.

Due to experimental reasons the unloaded pellets of aerosil could not be investigated in the fully dehydrated state. However it was already shown for related materials e.g., of AlMCM-41 [25], porous glass [26] or Anopore membranes [27] that the contribution of the nanoporous host material itself i.e., motions of the silica (or alumina) tetrahedra as building groups is negligibly small compared to that observed for the (liquid) filled samples. For instance the dielectric loss of AlMCM-41 molecular sieve is three orders of magnitude lower than that of a loaded sample and no loss peak could be observed in the spectra $\varepsilon'' - \log f$ for the unfilled sieve. On the other hand, the unusual dielectric behavior of water adsorbed into the pores of some silica molecular sieves [28] is an additional argument that the contribution of the pore wall material is negligible compared to that observed for the (liquid) filled samples. Therefore in the following the contribution of the aerosil to the dielectric loss of the composites is neglected.

3. Composite Aerosil-cyanophenyl Benzoate

Thermal Analysis

The final silica density was estimated by thermogravimetry. There are different reasons that both organic molecules and silica as well are lost in an uncontrolled way during the preparation of the composite. For instance aerosil can be removed by the applied vacuum together with the solvent. CP6B can be also evaporated. Therefore the composition of the prepared composites can be slightly different from the formulation. So the ratio of silica for 1 g of CP6B is 7.2 instead of planned 10. Using these data, the layer thickness is evaluated to 0.46 nm assuming a density of the layer of 1 g/cm^3 and a surface area of the composites of around 300 m^{2}g^{-1}: The number of monolayers in the surface layer was evaluated as well assuming a perpendicular anchoring (by the cyan group) of the CP6B molecules to the hydrophilic silica surfaces [1], based onto close size of the molecules. Thus, ca. 2 monolayers were supposed to exist.

Careful DSC measurements give no evidence for any phase transition appearing for the composite. This is expected because of the high disordering effects taking place for the composites: The orientational correlation of the molecules is destroyed for these samples with a high silica density.

FTIR Spectra

The interaction of the CP6B molecules with the silica surface depends on the intrinsic properties of both components. A strong LC anchoring at the particle surface is expected by hydrogen bonds between the cyan groups of the CP6B molecules and the hydroxyl groups of the silica surface, as it was found by IR spectroscopy for related composites based on 4-*n*-octyl-4′-cyanobiphenyl (8CB) [11]. In addition, the carbonyl group of CP6B molecules might interact with the surface OH groups as well. The IR spectrum of the composite with CP6B is presented in the Figure 2. This spectrum is complex and contains peaks due to both components.

It is known that cyan (nitrile) stretching region gives information on the molecules that are present in the composites: In the case of 4-*n*-pentyl-4′-cyanobiphenyl-silica-type composites, Zhou *et al.* [16] found three species: species in the “LC” state, species in a randomized state and hydrogen bonded species, in order of increasing wavenumbers. This assignment is suitable also in the CP6B case, taking into account the similitude of the adsorbed molecular group and the nature of the surface in both cases. In fact, the peaks in the CN stretching region are broader for the composite than for the bulk CP6B and shoulders are observed at higher wave numbers than for bulk CP6B (Fig. 6A). The decomposition into Gaussians [29] yields the position of the absorption peaks due to bulk-like CP6B and of these appearing at higher frequencies due to the interaction of the CN group with surface OH groups: 2227 cm^{-1} for bulk-like CP6B; 2231 cm^{-1} for "randomized" CP6B (sterically hindered to form H bonds); 2242 cm^{-1}

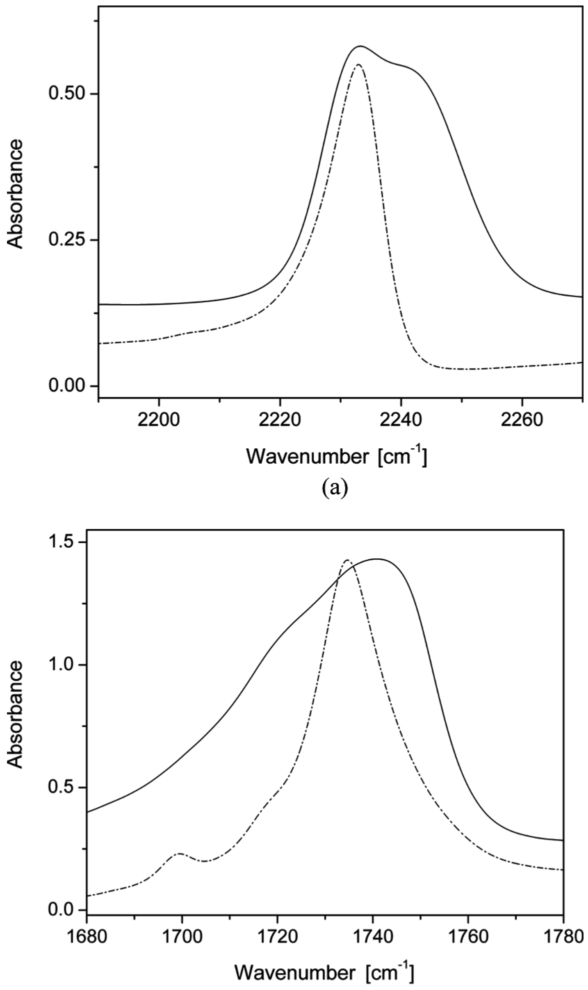

(a)

(b)

FIGURE 6 FTIR spectra in the region of cyan (a) and carbonyl (b) stretching vibration: solid line – composite; dashed-dotted line bulk CP6B.

for hydrogen bonded CP6B. Peak half-widths are broader for the composite than for bulk CP6B [29].

The CP6B molecules interact with the aerosil surface by ester group (Fig. 6B) too. This is put in evidence by the shift of the peak of the carbonyl stretching toward higher wavenumbers [29] and its significant broadening.

A wide characteristic band due to stretching vibrations of hydrogen bonded hydroxyl groups appears in the spectra at $\sim 3500\,\mathrm{cm}^{-1}$ (Fig. 2) also indicating that a part of the molecules are involved in hydrogen bonds. In conclusion by their features, these IR spectra show clearly that CP6B molecules strongly interact with the aerosil surface.

Dielectric Spectroscopy

Since CP6B molecules interact strongly with the silica surface it is expected that the molecular dynamics of the surface layer must be different than that of bulk CP6B. In Figure 7 the dielectric loss ε'' versus frequency and temperature is shown for the aerosil composite in a 3D representation. Only one relaxation process indicated by a peak in the dielectric loss is observed for the composite. The shift of the maximum of the dielectric loss toward higher frequencies with increasing temperature is shown in Figure 8 for some selected temperatures.

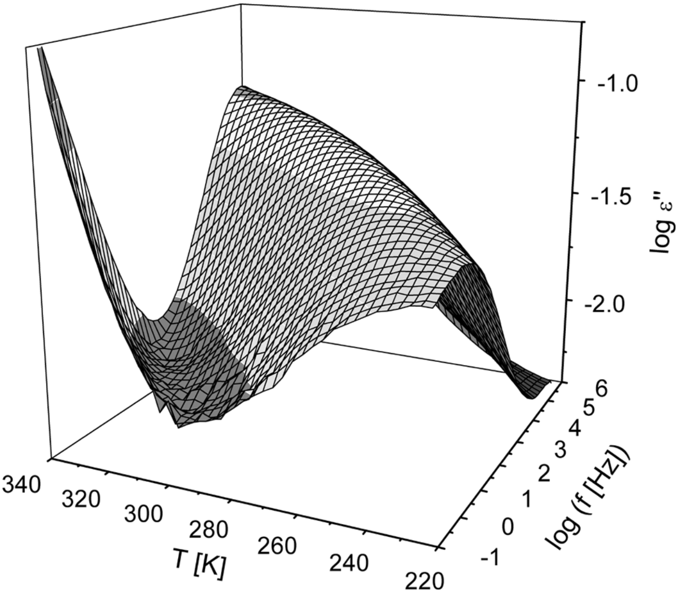

FIGURE 7 Dielectric loss of the composite vs. frequency and temperature in a 3D representation.

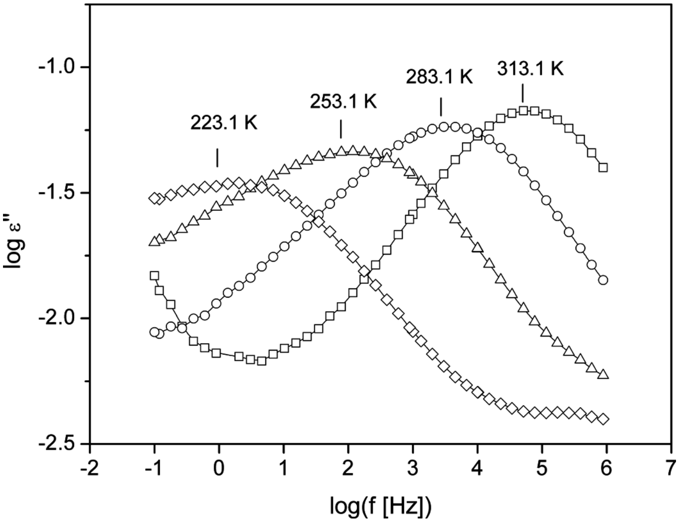

FIGURE 8 Dielectric loss of the composite vs. frequency for the labeled temperatures.

At low temperatures the loss peak is rather broad indicating a broad distribution of relaxation times. With increasing temperature the process becomes narrower. Assuming that the width of the loss peak is due to distribution of relaxation times, it results that the anchoring of the CP6B molecules to the surface of silica particles, become more homogeneous with increasing the temperature (see Fig. 8).

The dielectric loss given in Figures 7 and 8 correspond to temperatures of the isotropic, nematic and crystalline state of bulk CP6B. The temperature dependence of the relaxation rates of the surface layer is given in Figure 9. For all temperatures it is much lower than that of the corresponding bulk CP6B in both the nematic and the isotropic state. No discontinuities in the temperature dependence of the relaxation rates are observed at the phase transition of bulk CP6B (Fig. 9). Also the dielectric relaxation strength varies continuously with temperature with no discontinuities at the phase transition (see below). That gives additional evidence that the structure of the layer is maintained at the phase transition of the bulk LC.

Moreover an identical temperature dependence of the relaxation rates is found for heating and cooling (see Fig. 9). No hysteresis is observed, as it is typical for liquid crystals. For these reasons this relaxation process cannot be assigned either to the bulk CP6B or to

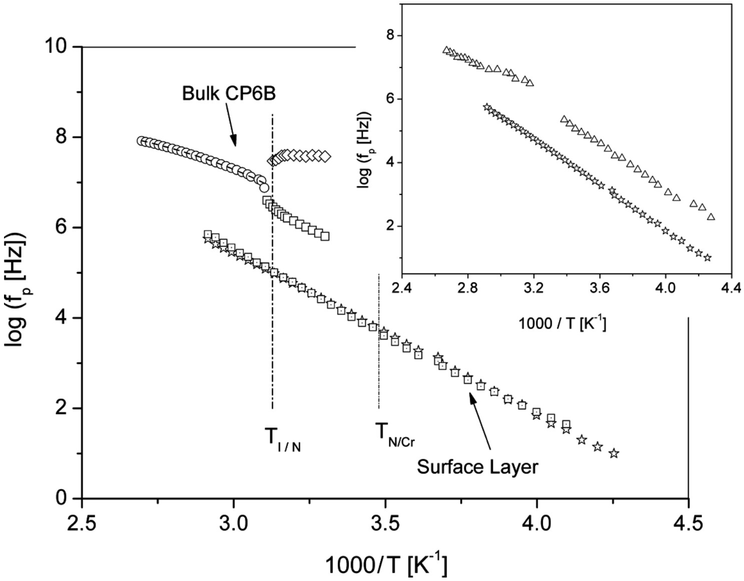

FIGURE 9 Relaxation rate f_p vs. inverse temperature for bulk CP6B and for the surface layer: Bulk CP6B: ○-isotropic state; □-δ-relaxation, ◇-tumbling mode. Surface layer: ☆-during heating; ⊡-during cooling. The phase transition temperatures are taken from the DSC experiments during cooling. The inset compares the temperature dependence of the relaxation rates for the composites containing CP6B (☆) and 6CB (△).

the pure aerosil, it is observed only for the composite system. Since in the composite, the CP6B molecules are located mostly in a surface layer, this slow relaxation process has to be assigned to a surface layer of CP6B molecules interacting with the silica particles.

The inset of Figure 9 compares the temperature dependence of the relaxation rate for the composite containing CP6B molecules with that for a composite containing the corresponding cyanobiphenyl 6CB in a similar concentration [7]. For the former the absolute values of the relaxation rates are by more than one order of magnitude lower than in the case of 6CB. This can be understood on the base of the stronger interaction of the CP6B molecules with the surface.

At the first glance the temperature dependence of the relaxation rates seems to be Arrhenius like. But applying the derivative technique also to the relaxation rates of the process observed for the composite the data in the plot $[d \log f_p/dT]^{-1/2}$ vs. T (Fig. 10) shows up as a straight line. This is an unambiguous proof that the temperature

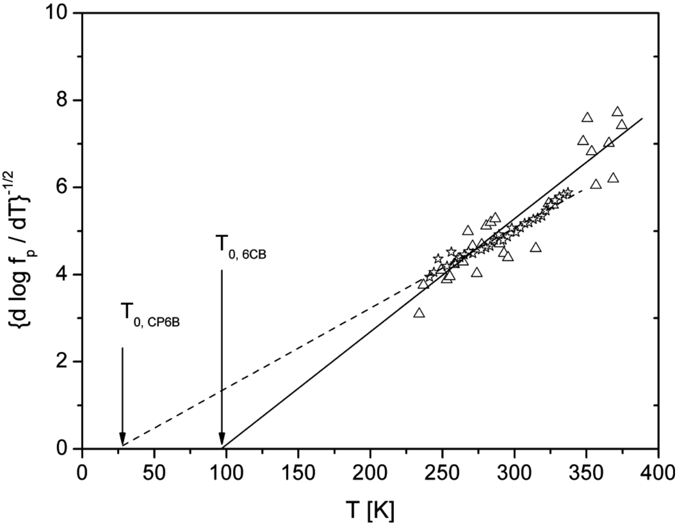

FIGURE 10 $(d\log f_p/dT)^{-1/2}$ vs. temperature for the surface layer: ☆-CP6B; △-6CB. The solid line is a linear regression to the data of 6CB. The dashed line is a linear regression to the data of CP6B.

dependence of the relaxation rates of the molecules in the surface layer follows a VFT-dependence. In general it is believed that a temperature dependence according to the VFT equation is a characteristic feature for glass-like dynamics. Therefore it is concluded that the molecular dynamics of the surface layer is quite similar to glassy dynamics. This conclusion is supported by the fact that $\Delta\varepsilon$ decreases with increasing temperature (see Fig. 11). This behavior is found also to be characteristic for such a process. For relaxation modes due to localized molecular fluctuations, usually the dielectric relaxation strength increases with increasing temperature. Because it was argued that the CP6B molecules form a surface layer on the silica with a nearly bi- or a monolayer structure, the investigated composite can be regarded as model systems with which to study glass transitions in a quasi two-dimensional system. A similar behavior was found for composites containing cynanobiphenyls in comparable concentration [7].

Figure 10 compares $[d\log f_p/dT]^{-1/2}$ versus T for composites containing CP6B and 6CB in a similar concentration. Although the data scatters a bit more for the 6CB case its temperature dependence can be also described by a straight line as for CP6B. The estimated Vogel temperature is by 60 K higher than that for the surface layer build of CP6B. CP6B is presumably longer than 6CB due to the ester

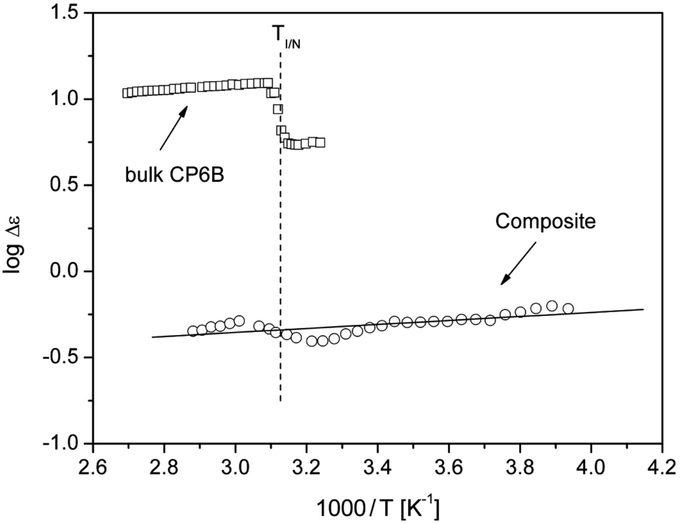

FIGURE 11 Dielectric strength for bulk CP6B (□, δ-relaxation) and for the composites (○).

bridge. It might be that for longer molecules the interactions with the surface which are responsible for the actual value of T_0 are screened out. For the cyanobiphenyl systems it is found that the Vogel temperature T_0 decreases with the length of the molecule in the surface layer [7 and references therein]. To confirm this also for the series of CPnB further experiments are necessary which are in preparation.

The relaxation of the molecules in the surface layer is a non-Debye process, much slower than that observed for bulk CP6B. Its relaxation rates have a temperature dependence governed by Vogel-Fulcher-Tammann law, which is characteristic for a glass forming liquid (the characteristic parameters are given in the Table 1). This behavior is in agreement with that observed for related composites containing cyanobiphenyls in controlled porous glass, Vycor glass or different membrane systems [26] and also found for composites containing molecular sieves with pores of/less than 2 nm [25]. It seems that the relaxation rate for the molecules in the outer surface layer is a bit higher (up to half-decade) than that for the molecules confined to the nanopores showing that these molecules experience less strong interactions than the confined ones. This is in accordance with the height of the potential "seen" by the molecule [30] resulting from the mean field theory of the LCs.

TABLE 1 VFT Parameters of the composite sample. For CP6B (isotropic state) and CP6B/A380 T_0 was estimated by the derivative technique. The prefactor and the A parameter were obtained by a fit of the VFT-equation to the relaxation rates keeping T_0 fixed

Sample	A [K]	T_0 [K]	log (f_p [Hz])	Reference
CP6B (isotropic state)	166.2	250	9.3	[23], this work
CP6B/A380	2996	24	15.1	This work
6CB (isotropic state)	168	225.6	9.3	[7]
6CB/A380	1718	81.7	13.6	[7]

CONCLUSIONS

Composites containing 4-hexyl-4′-cyanophenyl benzoate and aerosil particles were prepared having a silica density of ca. 7 g/cm^3. In accordance with previous estimations, under these conditions the amount of CP6B approaches nearly a surface layer consisting of two molecular sub-layers with high packing density. Strong anchoring of the CB molecules at the surface of aerosil particles by hydrogen bonds between the cyan and the ester group of the CP6B molecules and the hydroxyl groups of the aerosil surface was confirmed by FTIR measurements. Thus, band shape analysis show that most of the CP6B molecules form hydrogen bonds between their CN groups and surface OH groups.

A relaxation process was observed which has a much lower relaxation rate than the relaxation processes at lowest frequencies in the corresponding bulk CP6B in both the isotropic and the liquid crystalline nematic state. It can also be observed at temperatures were the CP6B is crystalline. Therefore it is assigned to molecular fluctuations of molecules located in a surface layer. The temperature dependence of the relaxation rates was analysed in detail using a derivative technique. It was shown that the temperature dependence of the estimated relaxation rate of the motional process due to the surface layer obeys a VFT law. It is generally believed that such a temperature dependence is a characteristic of glassy dynamics. Therefore it is argued that the investigated composites are model systems for studying the glass transition in quasi two-dimensional systems.

A detailed comparison was made with the relaxation of comparable cyanobiphenyl molecules with 6 carbon atoms in the alkyl chain adsorbed onto the same silica with a similar concentration.

REFERENCES

[1] Frunza, S., Frunza, L., Goering, H., Sturm, H., & Schönhals, A. (2001). *Europhys. Lett.*, *56*, 801.

[2] Hoffmann-La Roche & Co Ltd., Basel Switzerland, (1983). RO-CE-1510 Product Information.

[3] Titov, V. V., Kovshev, E. I., Pavluchenko, A. I., Lazareva, V. T., & Grebenkin, M. F. (1975). *J. Phys. (Paris), Suppl.*, *36*(C1), 387.

[4] Ivashchenko, A. V., Titov, V. V., & Kovshev, E. I. (1976). *Mol. Cryst. Liq. Cryst.*, *33*, 195.

[5] Karamysheva, L. A., Kovshev, E. I., & Barnik, M. I. (1976). *Mol. Cryst. Liq. Cryst.*, *37*, 29.

[6] Bykova, V. V., Burylin, P. A., Agafonova, I. S., & Maidachenko, G. G. (1991). *Izv. Vyssh. Uchebn. Zaved., Khim. Khim. Tekhnol.*, *34*, 85.

[7] Frunza, S., Frunza, L., Tintaru, M., Enache, I., Beica, T., & Schönhals, A. (2004). *Liq. Cryst.*, *31*, 913.

[8] Frunza, L., Schönhals, A., Frunza, S., Parvulescu, V. I., Cojocaru, B., Carriazo, D., Martín, C., & Rives, V. (2007). *J. Phys. Chem. A*, *111*, 5166.

[9] Kremer, F. & Schönhals, A. (Eds.). (2003). *Broadband Dielectric Spectroscopy*, Springer-Verlag: Berlin-Heidelberg, (a) 35 ff; (b) 59 ff; (c) 392; (d) 99 ff; (e) 171ff.

[10] Frunza, S., Kosslick, H., Schönhals, A., Frunza, L., Enache, I., & Beica, T. (2003). *J. Non-Cryst. Solids*, *325*, 103.

[11] Frunza, L., Frunza, S., Enache, I., Beica, T., Schönhals, A., Kosslick, H., Bentrup, U., & Pitsch, I. (2004). *Mol. Cryst. Liq. Cryst.*, *416*, 239.

[12] Laeri, F., Schueth, F., Simon, U., & Wark, M. (Eds.). (2003). *Host-Guest Systems Based on Nanoporous crystals*, Wiley-VCH: Weinheim, 84ff.

[13] Zubowa, H.-L., Kosslick, H., Carius, E., Frunza, S., Frunza, L., Landmesser, H., Richter, M., Schreier, E., & Fricke, R. (1998). *Micropor. Mesopor. Mater.*, *21*, 467.

[14] Frunza, L., Frunza, S., Schönhals, A., Zubowa, H.-L., Kosslick, H., & Fricke, R. (2000). *J. Mol. Struct.*, *563–564*, 491.

[15] (a) Gnatyuk, I., Puchkovskaya, G., Yaroshchuk, O., Goltsov, Y., Matkovskaya, L., Baran, J., Morawska-Kowal, T., & Ratajczak, H. (1999). *J. Mol. Struct.*, *512*, 189. (b) Gavrilko, T., Gnatyuk, I., Puchkovskaya, G., Goltsov, Yu., Matkovskaya, L., Baran, J., Drozd, M., & Ratajczak, H. (2000). *Vibr. Spectr.*, *23*, 199. (c) Gnatyuk, I., Gavrilko, T., Puchkovska, G., Chashchnikova, I., Baran, J., & Ratajczak, H. (2002). *J. Mol. Struct.*, *614*, 233.

[16] (a) Zhou, Y. W., Jaroniec, M., & Gilpin, R. K. (1994). *Anal. Chem.*, *66*, 4100. (b) Zhou, Y. W., Jaroniec, M., Hann, G. L., & Gilpin, R. K. (1994). *Anal. Chem.*, *66*, 1454.

[17] Leyte, J. C., Jesse, W., Leyte-Zuiderweg, L. H., & van Woerkom, P. C. M. (1998). *J. Phys.: Condens. Matter.*, *10*, 11617.

[18] Czarnecki, M. A., Okretic, S., & Siesler, H. W. (1997). *J. Phys. Chem. B*, *101*, 374.

[19] Cross, S. N. W. & Rochester, C. N. H. (1981). *J. Chem. Soc., Faraday Trans. 1*, *77*, 1027.

[20] (a) Jazdyn, J., Legrand, C., Czechowski, G., & Bauman, D. (1998). *Liq. Cryst.*, *24*, 689. (b) Jadzyn, J., Czechowski, G., Douali, R., & Legrand, C. (1999). *Liq. Cryst.*, *26*, 1591.

[21] (a) Vogel, H. (1921). *Phys. Zeit.*, *22*, 645. (b) Fulcher, G. S. (1925). *J. Am. Ceram. Soc.*, *8*, 339. (c) Tammann, G. & Hesse, G. (1926). *Anorg. Allgem. Chem.*, *156*, 245.

[22] (a) Zeller, H. R. (1982). *Phys. Rev. Lett.*, *48*, 334. (b) Benguigui, L. (1984). *Phys. Rev.*, *A28*, 1852; idem. (1984). *Phys. Rev., A*, *29*, 2968; idem. (1983). *Mol. Cryst. Liq.*

Cryst., *114*, 51. (c) Diogo, A. C. & Martins, A. F. (1982). *J. Phys. (Paris)*, *43*, 779. (d) Brás, A. R., Dionisio, M., Huth, H., Schick, Ch., & Schönhals, A. (2007). *Phys. Rev. E*, *75*, 061708.

[23] Frunza, S., Frunza, L., & Schönhals, A. (2008). under preparation.

[24] Iannacchione, G. S., Garland, C. W., Mang, J. T., & Rieker, T. P. (1998). *Phys. Rev. E*, *58*, 5966.

[25] Frunza, S., Schönhals, A., Frunza, L., Zubowa, H.-L., Kosslick, H., Fricke, R., & Carius, H. (1999). *Chem. Phys. Lett.*, *307*, 167.

[26] (a) Crandall, K. A., Rosenblatt, C., & Aliev, F. M. (1996). *Phys. Rev. E*, *53*, 96. (b) Iannacchione, G. S., Qian, S., Finotello, D., & Aliev, F. M. (1997). *Phys. Rev. E*, *56*, 554. (c) Arcioni, A., Bacchiocchi, C., Grossi, L., Nicolini, A., & Zannoni, C. (2002). *J. Phys. Chem. B*, *106*, 9245. (d) Sinha, G. P. & Aliev, F. M. (1998). *Phys. Rev. E*, *58*, 2001. (e) Hourri, A., Jamee, P., Bose, T. K., & Thoen, J. (2002). *Liq. Cryst.*, *39*, 459.

[27] Rozanski, S. A., Stannarius, R., Groothues, H., & Kremer, F. (1996). *Liq. Cryst.*, *20*, 59.

[28] Frunza, L., Kosslick, H., Pitsch, I., Frunza, S., & Schönhals, A. (2005). *J. Phys. Chem. B*, *109*, 9154.

[29] Frunza, L., Poterasu, M., & Frunza, S. (2008). under preparation.

[30] Kreul, H. G., Urban, S., & Wurflinger, A. (1992). *Phys. Rev. A*, *45*, 8624.